Sangbin Lee[®], Qi Jian Lim[®], Charles Ross[®], Eungkyu Lee[®], Soyul Han, Youngmin Kim, Zhen Peng[®], and Sanghoek Kim[®]

Quantum Annealing for Electromagnetic Engineers—Part I

A computational method to solve various types of optimization problems.

XXXX

t is well known that electromagnetic computations are computationally demanding. Interestingly, many such problems can be recast to be solved by quantum annealing. Quantum annealing, a kind of quantum computer, utilizes quantum tunneling for state transitions, which enables one to find the global minimum in a complex energy landscape. Part I of this article explains quantum annealing for the classical electromagnetic community, assuming little knowledge of quantum theory. It reviews the basic principle and recent advances in quantum annealing to extend its applications, such as a hybrid quantumclassical annealing algorithm. Part II presents various examples of electromagnetic problems that can be solved by quantum annealing. These are 1) optimization of a reconfigurable directional metasurface, 2) finding current distribution in an arbitrary wire antenna, 3) finding charge and field distributions in a static condition, and 4) optimization of source excitation to focus fields in hyperthermia. Lastly, the performance of the quantum

annealer is compared with classical solvers to deduce the type of applications in which a quantum annealer of current technologies can be preferred in practice.

INTRODUCTION

Quantum computing is one of the most rapidly advancing research fields, aspiring to conquer intractable computational problems that have long perplexed classical computers, exemplified by the prime factorization of significantly large numbers [1], unstructured search problems [2], and the simulation of quantum mechanical phenomena [3]. Technically, any such quantum algorithm can run on *gate-based* universal quantum computers, which are founded on a set of quantum logical gates. Depending on how the quantum bits (or *qubits*), the fundamental information carrier in a quantum computer, are realized, there are three leading technologies of a gate-based quantum computer: trapped-ion qubits, semiconductor-spin qubits, and superconducting-circuit qubits. Despite its versatility in computation, however, the gate-based quantum computer requires

Digital Object Identifier 10.1109/MAP.2024.3498695

critical innovations before it can achieve quantum supremacy. For example, while it is estimated to require a million-qubitscale system to realize a practical universal system, the largest gate-based quantum computer so far has only 127 qubits [4].

On the other hand, quantum annealing is an adiabatic quantum computer that finds the global minimum of a given objective function over a set of candidate states by the process of quantum fluctuations. In contrast to the gate-based quantum computer, quantum annealing is specialized to handle certain types of optimization, such as combinatorial optimization problems. Regardless of its relatively limited applications, quantum annealing remains an enticing solution due to its intrinsic fault tolerance [5], which provides a competitive edge in developing a large-scale quantum computer. The potential of large-scale quantum computers becomes apparent when comparing the number of qubits for state-of-the-art quantum computers using the two methods. Currently, D-Wave's annealing solver, one of the most widely adopted quantum annealers, has 5,640 qubits [6], much larger than the gate-based counterpart.

Harnessing its relatively large scale for reflecting a practical system, quantum annealing has been successfully applied to various fields, including finance [7], machine learning [8], and cryptography [9] as well as optical [10] and microwave [11], [12] system designs. Noting its significant impact across a wide range of fields, including electromagnetism, Part I of this article introduces the fundamentals of quantum annealing to the electromagnetic community, assuming little knowledge of readers on quantum physics. The quantum annealing process is illustrated through numerical examples, facilitating the readers' comprehension of it. This allows one to discern the types of problems to which quantum annealing is applicable. At the end of Part I, we introduce recent advancements in quantum annealing methods for handling complex and large-scale problems.

PRINCIPLES OF QUANTUM ANNEALING

This section explains the basic principles of quantum annealing. To understand quantum annealing, it is necessary to review some properties of quantum mechanics. This section briefly explains these essential properties of quantum mechanics along with the principles of quantum annealing.

QUBIT

In quantum annealing (or quantum computers in general), the qubit acts as an information carrier, as the logical bit does in classical computers. Unlike the logical bit with a state of either zero or one, the qubit can be in a superposition of its zero or one state. The zero and one states are called the *energy states* because they have distinct energy values, say E_0 and E_1 , and are denoted as kets $|0\rangle$ and $|1\rangle$ in the bra-ket notation, respectively. The instantaneous state, $|\psi\rangle$, of a qubit in a linear superposition of two energy states is described as

$$|\psi\rangle = \alpha_0|0\rangle + \alpha_1|1\rangle = \begin{bmatrix} \alpha_0\\ \alpha_1 \end{bmatrix}.$$
 (1)

Since any qubit state can be expressed as a linear summation of $|0\rangle$ and $|1\rangle$, $\{|0\rangle, |1\rangle\}$ is a basis of the vector space of the qubit state. When measuring the state of qubits, they collapse to one of their energy states. This collapse is a probabilistic process, where the probability of collapsing to $|0\rangle$ and $|1\rangle$, denoted as $P_{|0\rangle}$ and $P_{|1\rangle}$, can be obtained from the inner product with a corresponding *bras*, $\langle 0|$ and $\langle 1|$ —for example, $P_{|0\rangle} = |\langle 0|\psi \rangle|^2 = |\alpha_0|^2$, where the orthonormality of the basis is used in the second equality. Likewise, $P_{|1\rangle}$ is given by $|\alpha_1|^2$. This is why the complex coefficients, α_0 and α_1 , are often called *probabil*ity amplitudes. Since the state should always be measured as either zero or one, the complex coefficients satisfy $|\alpha_0|^2 + |\alpha_1|^2 = 1$.

HAMILTONIAN OPERATOR Ĥ

In quantum physics, every physical observation is associated with a Hermitian operator. In other words, the measurement result of a physical observation must be an eigenvalue of the corresponding Hermitian operator. For instance, one can find an operator associated with the position, another operator with the momentum, and yet another operator with the energy, and so on.

In particular, the operator associated with the energy, called Hamiltonian \hat{H} , is of greatest interest in quantum annealing. Following the physicists' convention, the hat symbol (î) above the character represents it as an operator in this article. The reason why the Hamiltonian is essential in quantum annealing is because quantum annealing exploits quantum physics to find the lowest-energy state of qubits. It recasts an optimization problem of interest to the energy minimization problem of which the minimum solution can be naturally obtained from quantum physics. Since the Hamiltonian is used to obtain the energy of a state, it is the most important operator in quantum annealing. The Hamiltonian \hat{H} is also important because it describes how the state should change with time

$$i\hbar \frac{\partial}{\partial t} |\psi\rangle = \hat{H} |\psi\rangle.$$
 (2)

Alternatively, using the right-hand side of (1), the previous equation may be rephrased as

$$i\hbar \frac{\partial}{\partial t} \begin{bmatrix} \alpha_0 \\ \alpha_1 \end{bmatrix} = H \begin{bmatrix} \alpha_0 \\ \alpha_1 \end{bmatrix} \tag{3}$$

where H without the hat symbol $(\hat{\cdot})$ is the matrix representation of the \hat{H} operator in the basis of $\{|0\rangle, |1\rangle\}$. To help readers get familiar with the Hamiltonian, let's consider the Hamiltonian of a single qubit of which the energy is definite; i.e., the energy level does not change with time. Since the energy level does not change with time, one may attempt to regard the left-hand side of (3) as zero, leading to the Hamiltonian matrix being the zero matrix. Instead, in quantum mechanics, while the magnitude of the probability amplitude of a particle in a state of definite energy E_0 is static, its phase changes with time as $e^{-i(E_0/\hbar)t}$ [13]. For α_0 and α_1 with the time dependency of $e^{-i(E_0/\hbar)t}$ and $e^{-i(E_1/\hbar)t}$ to satisfy (3), the Hamiltonian for a single qubit with a definite energy has the matrix expression of

$$H = \begin{bmatrix} E_0 & 0\\ 0 & E_1 \end{bmatrix}. \tag{4}$$

Indeed, note that the eigenvalues of the Hamiltonian operator, which are independent of the choice of the basis, correspond to the energy. In general, the Hamiltonian, which is a 2×2 Hermitian matrix, is spanned by four bases $\{I, \sigma_x, \sigma_y, \sigma_z\}$, where I is the identity matrix and the other three matrices are the *Pauli matrices*

$$\sigma_x \equiv \begin{pmatrix} 0 & 1 \\ 1 & 0 \end{pmatrix}, \quad \sigma_y \equiv \begin{pmatrix} 0 & -i \\ i & 0 \end{pmatrix}, \quad \sigma_z \equiv \begin{pmatrix} 1 & 0 \\ 0 & -1 \end{pmatrix}.$$
 (5)

For example, the Hamiltonian H of (4) can be expressed as $H = 1/2[(E_0 + E_1)I - (E_1 - E_0)\sigma_z]$.

THE SIMPLEST QUANTUM ANNEALER: A SINGLE-QUBIT QUANTUM ANNEALER

Equipped with the knowledge of the qubit and the Hamiltonian, we can now understand the operation of the simplest quantum annealer, which consists of a single qubit. Assume that we want to solve the following optimization problem:

Find
$$x \in \{-1, 1\}$$
 that minimizes $F = Qx \ (0 \le Q \in \mathbb{R})$. (6)

This is a toy problem of which the solution is trivial; x=-1 to minimize the cost function to $F_{\min}=-Q$. Nevertheless, we want to use this simple problem to illustrate how the quantum annealer operates to find the optimal solution. First of all, the cost function F is equivalent to the energy eigenvalue of the Hamiltonian $H_1=[-Q,0;0,Q]$. In other words, the state's energy is -Q when the qubit is in $|0\rangle$ state and Q when the qubit is in $|1\rangle$ state. The objective is equivalent to minimizing the energy of the state with the Hamiltonian $\hat{H}_1=-Q\hat{\sigma}_z$.

To avoid being trapped in a local minimum, quantum annealing starts from a superposition of all possible states with equal weights. For a single qubit, for instance, we want to set the initial state to be $|\psi_0\rangle=1/\sqrt{2}\,(|0\rangle+|1\rangle)$. For this purpose, the initial Hamiltonian is set to be $\hat{H}_0=-\hat{\sigma}_x$. Physically, this can be set by applying an external magnetic field to the qubit [14], [15]. Interested readers may refer to "Hardware Implementation of Quantum Annealer" for details. The initial Hamiltonian \hat{H}_0 has two distinct energies (eigenvalues) -1 and 1, with the corresponding eigenstates of $|\psi_0\rangle=1/\sqrt{2}\,(|0\rangle+|1\rangle)$ and $|\psi_1\rangle=1/\sqrt{2}\,(|0\rangle-|1\rangle)$. Since the quantum annealer sets the temperature of the system sufficiently low (a few tens of milli-Kelvin), the qubit is in the lowest-energy (ground) state: $|\psi\rangle=|\psi_0\rangle$.

After the initial setup, the external magnetic field slowly changes to convert the Hamiltonian from \hat{H}_0 to \hat{H}_1 . For example, the Hamiltonian of the system at time $t(0 \le t \le t_f)$, $\hat{H}(t)$ changes with time as

$$\hat{H}(t) = \frac{t_f - t}{t_f} \hat{H}_0 + \frac{t}{t_f} \hat{H}_1 \tag{7}$$

where t_f is the time duration during which the conversion occurs. If the Hamiltonian is converted slowly enough, the system's state can retain the lowest energy state throughout the annealing process. How slowly should it be converted?

According to the *adiabatic theorem* in quantum mechanics, the rate of change of the Hamiltonian must be sufficiently lower than the gap between the lowest and the second-lowest energy spectrum [16]. If this adiabatic condition is met, the qubit will still be in the lowest energy state of \hat{H}_1 when the annealing is finished at $t=t_f$, which is $|0\rangle$ corresponding to the minimum energy of -Q. This is the correct result of minimization: $F_{\min} = -Q$.

MULTIPLE QUBITS

In practice, a quantum computer comprises multiple qubits. The states of multiple qubits form a new vector space and can be constructed from the vector spaces of individual qubit states using the *tensor product*, denoted by \otimes . For instance, an instantaneous state $|\psi\rangle$ of two qubits can be expressed as $|\phi\rangle_1\otimes|\xi\rangle_2$, where $|\phi\rangle_1$ and $|\xi\rangle_2$ refers to the state of the first and second qubits, respectively.

To understand the vector space of multiple qubit states, it is essential to figure out the basis of the vector space. The basis of, say, a two-qubit vector space can be constructed as follows. When the states of two qubits are measured, each should collapse to one of their energy states: either $|0\rangle$ or $|1\rangle$. Explicitly, labeling the basis of qubit I's state as $\{|0\rangle_1, |1\rangle_1\}$ and qubit 2's state as $\{|0\rangle_2, |1\rangle_2\}$, the basis of two-qubit states consists of $\{|0\rangle_1 \otimes |0\rangle_2$, $|0\rangle_1 \otimes |1\rangle_2$, $|1\rangle_1 \otimes |0\rangle_2$, $|1\rangle_1 \otimes |1\rangle_2$, often labeled as $\{|00\rangle, |01\rangle, |10\rangle, |11\rangle\}$ for brevity. This implies, in general, that an instantaneous state $|\psi\rangle$ of two qubits can be expressed as $|\psi\rangle = \alpha_0|00\rangle + \alpha_1|01\rangle + \alpha_2|10\rangle + \alpha_3|11\rangle$, where the complex coefficients are the probability amplitudes, representing the probability that the qubits are measured to be the corresponding state; e.g., $P_{|10\rangle} = |\langle 10 | \psi \rangle|^2 = |\alpha_2|^2.$

Likewise, in a quantum computer with N qubits, the state of the whole qubits is the superposition of 2^N energy states. The 2^N energy states forming the basis of N-qubit states are $\{|0...00\rangle, |0...01\rangle, ..., |1...11\rangle\}$. Mathematically, the instantaneous state of N multiple qubits is the superposition of the basis as

$$|\psi\rangle = \alpha_0 |0...00\rangle + \alpha_1 |0...01\rangle + ... + \alpha_{2^{N}-1} |1...11\rangle$$

$$= \begin{bmatrix} \alpha_0 \\ \alpha_1 \\ \vdots \\ \alpha_{2^{N}-1} \end{bmatrix}$$
(8)

where $\sum_{i=0}^{2^{N}-1} |\alpha_{i}|^{2} = 1$.

Operators acting in the vector space of multiple qubits can also be constructed by the tensor product with the same symbol \otimes . For a two-qubit system, for example, let \hat{A} be an operator acting on the state $|\phi\rangle_1$ of the first qubit and \hat{B} be an operator acting on the state $|\xi\rangle_2$ of the second qubit. We can construct the operator $\hat{A}\otimes\hat{B}$ for a two-qubit state defined to act as follows [17]:

$$\hat{A} \otimes \hat{B}(|\phi\rangle_1 \otimes |\xi\rangle_2) \equiv (\hat{A}|\phi\rangle_1) \otimes (\hat{B}|\xi\rangle_2). \tag{9}$$

HARDWARE IMPLEMENTATION OF QUANTUM ANNEALER

This tutorial article mainly discusses the mathematical modeling of quantum annealing to understand how it works. Although the hardware implementation of the quantum annealer is out of the scope of this tutorial article, we briefly cover it in this sidebar. In short, it is about how the qubit is implemented and how the coefficients Q_i for individual qubits and Q_{ii} for the interaction between gubits in (14) are physically manipulated.

How is the Qubit Implemented in Quantum Annealer?

As stated in the "Introduction" section, qubits are being implemented in various ways for the gate-based quantum computer. For quantum annealing, on the other hand, there is a prominent method to implement it, which is to use a superconducting loop, as shown in Figure S1(a).

Why do we need a superconductor for quantum annealing in the first place? That is because we want to invoke quantum mechanical behavior on a macroscopic scale. In general, we can measure the phenomena on the macroscopic scale very well, such as the current or charge amount, in which billions of electrons are typically engaged. The critical problem is that the electron is a fermi particle, which means that there can be at most one electron for each state, making the observation of its quantum behavior extremely difficult.

If a conductor turns into a superconductor, things change in a very intriguing way other than that its resistivity goes to zero. When it becomes a superconductor, two electrons form a bound pair called the Cooper pair. Interestingly, this pair does not act like a fermi particle but does act like a boson particle, meaning that they like to be in the same state.

Returning to our story of the quantum annealer, we need many particles, whether they are electrons or Cooper pairs, to be in the lowest energy state to enable the measurement on a macroscopic scale. In a superconductor at a very low temperature, all the electrons turn into the Cooper pairs, and all the Cooper pairs are technically occupied in the lowest state, enabling the measurement. This is why we want to use a superconductor despite the pain of lowering the operation temperature.

How Do We Control the Q_i for an Individual Qubit, A(T), and B(T)?

A superconducting flux qubit consists of a main loop and a small loop interrupting in the middle of the main one, as seen in Figure S1(a). Notice that there are two thin insulators on the small loop, called the Josephson junction, which is another key element in the superconducting flux qubit. The main loop can support two current flows [15], clockwise and anticlockwise circulating currents, effectively representing quantum binary states $|0\rangle$ and $|1\rangle$, respectively. The Josephson junction allows a small chance of flip-flopping the current direction and of changing a superposition state between $|0\rangle$ and $|1\rangle$.

The probability amplitudes of the states can be effectively controlled by changing the external magnetic flux to the main loop, denoted as Φ_{1x} . In quantum mechanics, the flux entering into a superconducting coil is quantized in units of the flux *quantum* Φ_0 . When the external flux Φ_{1x} is given as half of the flux quantum $\Phi_0/2$, the flux through the main loop may or may not exist with a 50/50 chance, implying that the gubit state is $|\psi_0\rangle = 1/\sqrt{2} (|0\rangle + |1\rangle)$. From the perspective of the Hamiltonian, it means that $\hat{H}_0 = -\hat{\sigma}_{x_f}$ and from the perspective of the energy landscape, it means that the energy levels of $|0\rangle$ and $|1\rangle$ are equally low, as shown in Figure S1(b) (left). This is the initial state of the qubit in the quantum annealing, in which $A(t) \gg B(t)$ and $\hat{H}(t) \approx \hat{H}_0(t)$.

When the external magnetic flux Φ_{1x} changes, it changes the energy landscape. One of the current directions may have a lower potential energy due to the nonzero $(\Phi_{1x} - \Phi_0/2)$, tilting the landscape as in Figure S1(b) (center) and Figure S1(b) (right) by time. This shows that the external magnetic flux Φ_{1x} determines the energy difference 2 h between two minima [Figure S1(b) (center)]. The qubit is more likely to be measured at a lower energy state than the other state, which is equivalent to introducing the term $-Q\hat{\sigma}_z$ in the Hamiltonian. In other words, by controlling the Φ_{1x} , one can manipulate B(t)/A(t) as well as Q_i for individual qubits.

Next, we want to discuss the role of the small loop and the magnetic flux Φ_2 into it. During the transition from the initial to the final Hamiltonian, the energy barrier δU between the two states may appear high. If this barrier height appears too high before the energy difference is given, the state may be trapped in a local minimum, failing to reach the global minimum at the end of the annealing process. We want to suppress the rise of the barrier δU until the energy difference is sufficiently applied. The two Josephson junctions and the magnetic flux Φ_2 can handle this. One can show that the barrier height δU depends on Φ_2 as [S1]

(Continued)

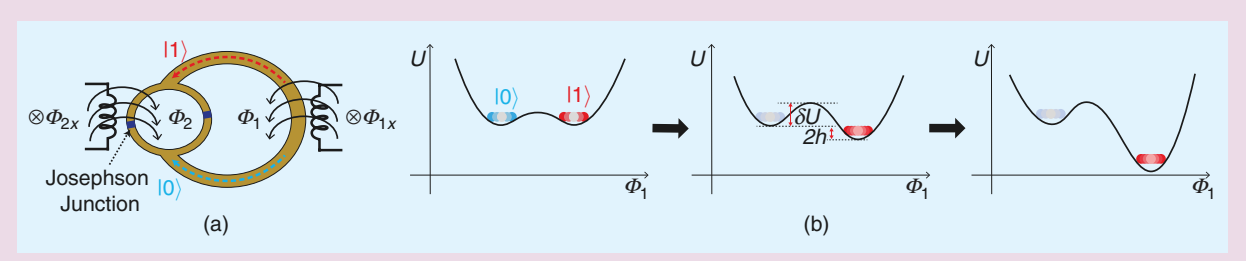


FIGURE 51. (a) A schematic of a superconducting flux qubit. (b) The evolution of the qubit energy diagram along the annealing schedule.

HARDWARE IMPLEMENTATION OF QUANTUM ANNEALER (Continued)

$$\delta U \propto \cos \frac{\pi \Phi_2}{\Phi_0}$$
. (S1)

Therefore, by controlling the magnetic flux Φ_2 from the external flux Φ_{2x} , one can manipulate the barrier height δU as necessary and avoid falling in a local minimum.

How to Control the Q_{ii} ?

The programmable Q_{ij} in (14) is physically synthesized by a block named the *coupler*. The coupler is based on the superconducting loop with the Josephson junctions [14], similar to the qubit design. Figure S2 shows an example of the coupler, in which the main loop is mutually coupled to two qubits. In the discussion of barrier height control in a single qubit, we have seen that a pair of Josephson junctions on a small loop plays the role of a *switch*, in the sense that it controls the isolation (the barrier height), depending on the magnetic flux into the loop. Similarly, the magnetic flux $\Phi_{co,x}$ into the small loop of the coupler can control the net current and affect the coupling between the qubits. In addition, the magnetic flux $\Phi_{act,x}$ into the main loop of the coupler tunes the spin-spin coupling energy between ferromagnetic and antiferromagnetic coupling, which is equivalent to deciding the sign and the amplitude of Q_{ii} .

Potential Error Sources in Quantum Annealer

Controlling individual qubits and their interactions accurately is quite challenging due to the numerous potential errors that can affect the quantum annealer. To list a few error sources, the qubit state may be excited unexpectedly by violating the quantum adiabatic condition or absorbing the thermal energy from the environment. Moreover, the biasing circuit of the qubit is susceptible to an error from 1/f noise that can propagate to the qubit [S1], [S2]. Some errors may originate from the physical device

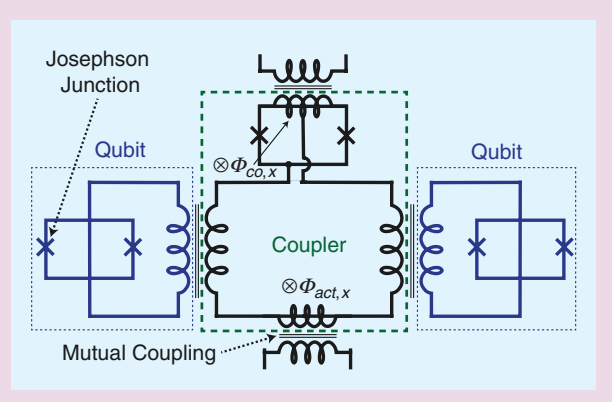


FIGURE S2. A schematic of a coupler between two qubits.

itself. For instance, some physical qubits may have a coupling-like effect that is not accounted for in the Hamiltonian formulation [14], [S1]. A truncation error may arise due to the finite resolution of the digital-to-analog converter that provides external flux to manipulate qubits. Aside from those, the result can be influenced by I/O systems and small variations in the physical properties of individual gubits [S3].

References

[S1] R. Harris et al., "Experimental demonstration of a robust and scalable flux qubit," *Phys. Rev. B*, vol. 81, no. 13, 2010, Art. no. 134510, doi: 10.1103/Phys-RevB.81.134510.

[S2] T. Lanting et al., "Geometrical dependence of the low-frequency noise in superconducting flux qubits," *Phys. Rev. B*, vol. 79, no. 6, 2009, Art. no. 060509, doi: 10.1103/PhysRevB.79.060509.

[S3] "Error sources for problem representation." D-Wave Systems Inc. Accessed: Nov. 23, 2024. [Online] Available: https://docs.dwavesys.com/docs/latest/c_qpu_ice.html

Note that the first \otimes symbol in (9) represents the tensor product between two operators, while the others represent the tensor products between the qubit states.

To grasp the tensor product between the operators better, let's consider the matrix representation of the operators $\hat{A} \otimes \hat{B}$ constructed from \hat{A} and \hat{B} . We further assume that their matrix representations are $A = [a_{11}, a_{12}; a_{21}, a_{22}]$ and $B = [b_{11}, b_{12}; b_{21}, b_{22}]$, both on the basis of energy states of each. The matrix element of the operator $\hat{A} \otimes \hat{B}$ can be found by mapping between bases via the operator. For example, one can check that $\langle 00|\hat{A} \otimes \hat{B}|00\rangle = a_{11}b_{11}$, which will be the matrix element at the first row and the first column. By repeating this process for every pair of bases, one can show that $\hat{A} \otimes \hat{B}$ has the representation of

$$A \otimes B = \begin{bmatrix} a_{11}b_{11} & a_{11}b_{12} & a_{12}b_{11} & a_{12}b_{12} \\ a_{11}b_{21} & a_{11}b_{22} & a_{12}b_{21} & a_{12}b_{22} \\ a_{21}b_{11} & a_{21}b_{12} & a_{22}b_{11} & a_{22}b_{12} \\ a_{21}b_{21} & a_{21}b_{22} & a_{22}b_{21} & a_{22}b_{22} \end{bmatrix}.$$
(10)

This 4×4 matrix represents the expanded operator $\hat{A} \otimes \hat{B}$ and acts on a 4×1 column vector representing the two-qubit state $|\psi\rangle = |\phi\rangle_1 \otimes |\xi\rangle_2$.

For a concrete example, we can consider the Hamiltonian operator $H_1 = [a_{11}, a_{12}; a_{21}, a_{22}]$ that acts on qubit 1 and $H_2 = [b_{11}, b_{12}; b_{21}, b_{22}]$ that acts on qubit 2. They can be upgraded to act on the two-qubit state as

$$H_1^{(1)} = H_1 \otimes I = \begin{bmatrix} a_{11} & 0 & a_{12} & 0 \\ 0 & a_{11} & 0 & a_{12} \\ a_{21} & 0 & a_{22} & 0 \\ 0 & a_{21} & 0 & a_{22} \end{bmatrix}$$
 (11)

$$H_2^{(2)} = I \otimes H_2 = \begin{bmatrix} b_{11} & b_{12} & 0 & 0 \\ b_{21} & b_{22} & 0 & 0 \\ 0 & 0 & b_{11} & b_{12} \\ 0 & 0 & b_{21} & b_{22} \end{bmatrix}.$$
(12)

These are some essential algebras to describe the operation of quantum annealing. Based on these, we shall see how the multiqubit quantum annealing works in the next section.

QUANTUM ANNEALING OF MULTIPLE QUBITS

Quantum annealing utilizes the natural evolution of a multiple-qubit quantum system to find the lowest energy solutions to a given Hamiltonian [18]. Generalizing the optimization problem that quantum annealing with a single qubit could solve in the "The Simplest Quantum Annealer: A Single-Qubit Quantum Annealer" section, quantum annealing with multiple qubits can solve the quadratic unconstrained binary optimization (QUBO) problems that are in the form of the following [19]:

Find
$$x_1, x_2, ..., x_N$$
 (where $x_i \in \{-1, 1\}$) that
minimizes $F = \sum_{i=1}^{N} Q_i x_i + \sum_{i=1}^{N} \sum_{j=i+1}^{N} Q_{ij} x_i x_j$ (13)

where Q_{ij} $(1 \le i \le j \le N)$ are real numbers. As we have done for the single qubit, one can show that the following Hamiltonian, called the Ising model, has the same energy spectrum as the cost function of the QUBO problem:

$$\hat{H}_{\text{ising}} = -\sum_{i=1}^{N} Q_i \hat{\sigma}_z^{(i)} + \sum_{i=1}^{N} \sum_{j=i+1}^{N} Q_{ij} \hat{\sigma}_z^{(i)} \hat{\sigma}_z^{(j)}$$
(14)

where the subscript and the superscript (i and j) denote the index of qubits. Note that each x_i is translated to $-\hat{\sigma}_z^{(i)}$ in the Ising model, which makes $x_i x_j$ translated to $+\hat{\sigma}_z^{(i)} \hat{\sigma}_z^{(j)}$. The coefficients Q_i are set in a physical annealer by applying the external magnetic field and Q_{ij} by creating the interaction between the ith and jth qubit [14]. Then, the lowest energy of the Ising Hamiltonian (14) matches with the minimum value of the QUBO problem in (13).

To reach the state of the minimum energy without being trapped in a local minimum, again the quantum annealer starts from an initial condition: $\hat{H}_0 = -\sum_{i=1}^N \hat{\sigma}_x^{(i)}$. The annealing schedule can be finely tuned to balance the simulation time and the risk of being trapped in a local minimum. Therefore, the Hamiltonian of the system can be generally expressed as

$$\hat{H}(t) = A(t)\hat{H}_0 + B(t)\hat{H}_{ising} \tag{15}$$

where A(t) and B(t) are the anneal fraction $(0 \le t \le t_f)$, abstract parameters to control the contribution of each Hamiltonian in time. When the quantum annealing schedule begins, A(t) is set to be much greater than B(t). Waiting to be cooled down, all the states are superposed with equal weights, which is our initial state. Next, the system monotonically decreases the contribution of the initial Hamiltonian, A(t), and increases the contribution of the final Hamiltonian, B(t). As B(t)increases, the probabilities of the superposed states start to differ [20]. Again, as explained in the "The Simplest Quantum Annealer: A Single-Qubit Quantum Annealer" section, such a transition should occur slowly so that the adiabatic theorem can ensure that the system retains the lowest energy [21]. By the end of the annealing schedule $(t = t_f)$, $A(t) \ll B(t)$, and the system would reach the state with the lowest energy of the Ising Hamiltonian.

NUMERICAL EXAMPLE OF QUANTUM ANNEALING

In this section, we show a numerical example to demonstrate how a multiqubit quantum annealer operates. Consider the following minimization problem:

Minimize
$$F = (x + y - 2)^2$$
, where $x, y \in \{-1, 1\}$. (16)

It is not as trivial as the optimization problem in (6), but it is still simple to find that the minimum solution F_{\min} is 0 when x = y = 1 at a glance. Since it has two binary variables, we need a two-qubit quantum annealer. Let's see how the twoqubit quantum annealer can handle this problem. First, we should prepare a superposed ground state with the initial Hamiltonian \hat{H}_0 . For two-qubit states, the initial Hamiltonian in the matrix representation with the basis of energy states is

$$H_{0} = -\sum_{i=1}^{2} \sigma_{x}^{(i)} = -\sigma_{x} \otimes I - I \otimes \sigma_{x}$$

$$= \begin{bmatrix} 0 & -1 & -1 & 0 \\ -1 & 0 & 0 & -1 \\ -1 & 0 & 0 & -1 \\ 0 & -1 & -1 & 0 \end{bmatrix}.$$
(17)

The initial Hamiltonian H_0 has the lowest eigenvalue of -2, and the corresponding eigenstate $0.5[1,1,1,1]^t$ is the superposition of all the eigenstates of $\hat{\sigma}_z$ with the equal weights. That is the initial state for the quantum annealing. To deduce the Ising Hamiltonian, one may ignore the constant terms (+4), including the square terms of the variable $(x^2 + y^2 = +2)$ The cost function F reduces to -4x - 4y + 2xy. Accordingly, the Ising Hamiltonian is

$$H_{\text{ising}} = 4(\sigma_z \otimes I) + 4(I \otimes \sigma_z) + 2(\sigma_z \otimes I)(I \otimes \sigma_z)$$

$$= \begin{bmatrix} 10 & 0 & 0 & 0 \\ 0 & -2 & 0 & 0 \\ 0 & 0 & -2 & 0 \\ 0 & 0 & 0 & -6 \end{bmatrix}.$$
(18)

During the quantum annealing process, the Hamiltonian evolves from H_0 to H_{ising} . Let's assume that A(t) decreases from one to zero and B(t) increases from zero to one in a linear manner from t = 0 to t_f . When (A(t), B(t)) = (0.7, 0.3), for example, H(t) is

$$H(t) = 0.7H_0 + 0.3H_{\text{ising}} = \begin{bmatrix} 3 & -0.7 & -0.7 & 0 \\ -0.7 & -0.6 & 0 & -0.7 \\ -0.7 & 0 & -0.6 & -0.7 \\ 0 & -0.7 & -0.7 & -1.8 \end{bmatrix}.$$
(19)

The lowest eigenvalue E_0 is -2.404 with the state $|\psi\rangle =$ $0.095|00\rangle + 0.367|01\rangle + 0.367|10\rangle + 0.850|11\rangle$. Other higher eigenvalues E_1 , E_2 , E_3 are -0.6, -0.26, and 3.27, respectively. Likewise, as the Hamiltonian changes from H_0 to H_{ising} during the time t_f , the eigenspectrum evolves as shown in Figure 1. Since there is no crossing point between E_0 and other eigenvalues, it satisfies the condition of the adiabatic process and is proper to be solved by the quantum annealer.

At last, when $t = t_f$, the Hamiltonian entirely changes to the Ising Hamiltonian, of which the lowest eigenvalue is -6 when the eigenstate is $[0,0,0,1]^t = |11\rangle$. Considering the omitted constant terms in the middle (=4+2=6), this is the correct minimal solution: $F_{\min} = 0$.

ADVANCES IN QUANTUM ANNEALING

In this section, we delve into several advanced topics concerning the utilization of quantum annealing methods for addressing complex large-scale optimization problems.

EXTENSION TO DISCRETE QUADRATIC MODELS

Although the spin states of variables on a quantum annealing device are binary, many tasks require optimizing variables over a discrete set of possible states that interact pairwise. These are called *discrete quadratic models* (DQMs) and are suitable optimization tasks for quantum annealing. Consider a DQM with N variables where the ith variable has m_i possible values. Its Hamiltonian is defined as follows:

$$\hat{H}_{\text{DQM}} = -\sum_{i=1}^{N} \sum_{u=1}^{m_i} Q_{iu} \hat{x}_z^{(i,u)} + \sum_{i=1}^{N} \sum_{j=i+1}^{N} \sum_{u=1}^{m_i} \sum_{v=1}^{m_j} Q_{ijuv} \hat{x}_z^{(i,u)} \hat{x}_z^{(j,v)}.$$
(20)

One method for encoding a DQM onto quantum annealing devices is via one-hot encoding [25]. In this approach, each discrete ith variable with m_i possible values is represented using m_i binary variables, all of which will be zero except for one, corresponding to the ideal discrete value. The overall Hamiltonian is

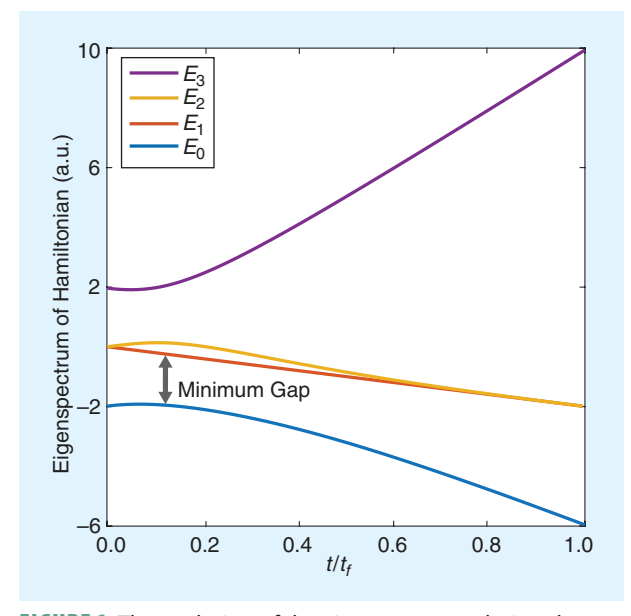


FIGURE 1. The evolution of the eigenspectrum during the annealing schedule. The eigenvalue E_0 of the smallest-energy state is denoted by the blue curve. It is lower than the other eigenvalues with the margin of the minimum gap shown in the figure. Such a gap is necessary for the quantum annealer to give a correct minimum solution. a.u.: arbitrary units.

$$\hat{H}_{\text{one-hot}} = \hat{H}_{\text{DQM}} + \lambda \sum_{i=1}^{N} \left(\sum_{u=1}^{m_i} \hat{x}_z^{(i,u)} - 1 \right)^2$$
 (21)

where λ is a suitably large penalty weight to impose the constraint that only a single binary variable may be equal to one for each discrete variable. The number of possible discrete states may vary with each variable. From this expression, it is evident that all binary variables that encode a discrete variable must interact with one another. This can make one-hot encoding inefficient when programming onto real quantum annealing devices.

As an alternative approach, the domain-wall encoding requires one fewer qubit per discrete variable and does not require that all binary variables that comprise a single discrete variable interact. In this method, the location of the domain wall (transition from -1 to +1) along a frustrated ferromagnetic spin chain encodes the value of the discrete variable. For a discrete variable with m possible values, the Hamiltonian of the Ising chain is given by

$$\hat{H}_{\text{chain}} = -\lambda \sum_{i=1}^{N} \sum_{u=0}^{m_i - 1} \hat{\sigma}_z^{(i,u)} \hat{\sigma}_z^{(i,u+1)}$$
(22)

where λ enforces a single domain wall along the chain, $\sigma_z^{(i,0)} = -1$, and $\sigma_z^{(i,m_i)} = 1$. Each binary variable is related to the spin variables on the chain, $x_z^{(i,u)} = 1/2(\sigma_z^{(i,u)} - \sigma_z^{(i,u-1)})$. The overall Hamiltonian is written as

$$\hat{H}_{\text{domain-wall}} = \hat{H}_{\text{DOM}} + \hat{H}_{\text{chain}}. \tag{23}$$

For example, encoding a discrete variable with four qubits using both one-hot and domain-wall encoding is shown in Table 1. The lower number of qubits and lack of complete coupling between constituent binary variables for each discrete variable allows domain-wall encoding to achieve superior theoretical and numerical performance.

HYBRID QUANTUM-CLASSICAL ANNEALING

Quantum annealing is a quantum computing paradigm designed to efficiently solve NP-hard optimization problems. It leverages quantum mechanics principles to explore the solution space and identify the optimal configuration for a given problem. In this approach, a quantum system is manipulated to evolve toward the solution of an optimization problem represented as the ground state of a Hamiltonian.

The state of the art in quantum computing is represented by noisy intermediate-scale quantum devices [26]. These devices have opened new avenues for tackling NP-hard problems, promising efficient solutions. For example, D-Wave stands out as a prominent participant in the quantum computing field, renowned for its pioneering quantum annealing technology. The company has achieved notable progress in advancing quantum computing technologies. As of the time of the crafting of this article, the D-Wave Advantage 4.1 quantum processing unit (QPU) [6] hardware showcases 5,640 functional qubits intricately connected through

a sparsely connected Pegasus topology and a technique called *minor embedding* [27]. However, despite these strides, D-Wave and comparable quantum machines continue to face challenges, including limitations in qubit quantity and connectivity. These challenges hinder their practicality in solving real-life problems [28] that demand a large number of densely connected qubits.

As a result, recent approaches for short- and medium-term solutions center on utilizing the combined advantages of classical and quantum computers. This blend of classical and quantum resources is a practical method to tackle the constraints posed by current quantum hardware and algorithms, particularly in handling large-scale optimization problems. To address this challenge, researchers employ *hybrid quantum-classical algorithms* [29], [30], [31], [32]. In this approach, classical computing power is employed for problem decomposition and integrating subsolutions. Quantum capabilities are then utilized to solve subproblems rapidly, optimizing overall computational efficiency.

One of the recent hybrid quantum-classical annealing algorithms is to utilize quantum annealing as a subsolver [33], inspired by the *large neighborhood search heuristic* algorithm [22], [23]. It concentrates on seeking local solutions within specific neighborhoods. These are essentially subsets or clusters of variables within the larger, more complex problem. In the proposed hybrid quantum-classical algorithm, this heuristic approach plays a crucial role in efficiently addressing the challenges posed by the intricate connectivity of qubits and the limited hardware resources.

The algorithm begins with classical resources identifying subproblems by defining neighborhoods within the overall problem space. These subproblems are then passed to the QPU for resolution using quantum annealing. Quantum annealing leverages quantum superposition and tunneling to rapidly explore and find optimal solutions for the local subproblems represented by the qubits. Once the quantum annealer completes its computations, the solutions for the subproblems are passed back to the classical machine. The classical component is responsible for merging these local solutions, thereby constructing a global solution for the entire problem. This iterative process of classical identification of subproblems, quantum resolution, and classical solution merging continues until the convergence criteria are met.

A compelling application of this algorithm is found in the domain of reconfigurable intelligent surface (RIS) beamforming optimization. In the specific context of RIS beamforming, the algorithm employs a fixed square frame that traverses the RIS surface (Figure 2). The algorithm optimizes the RIS elements within each frame using quantum annealing, rapidly seeking local solutions for that particular subregion. These locally optimized solutions are then amalgamated using classical computational resources to obtain the comprehensive and globally optimized solution for the entire RIS beamforming configuration. The combination of classical and quantum processing harnesses the strengths of both paradigms, enabling

more efficient and effective optimization for large and intricate problem instances.

UNCONSTRAINED AND CONSTRAINED QUADRATIC OPTIMIZATION PROBLEM

So far, we have seen that quantum annealing can solve QUBO problems. Since there is no other constraint that the variable should obey than that the variables have binary values, they are *unconstrained* problems. As long as the number of qubits permits, the quantum annealing can be further applied to solve an unconstrained quadratic optimization problem, also known as an unconstrained *quadratic programming* (*QP*) problem, in which variables can be real or even complex valued.

Because any real variable can be expressed as a string of binary variables with arbitrary precision, the unconstrained QP problem can ultimately boil down to the QUBO. There is a tradeoff between the truncation error and the length of the binary string to represent real variables. The latter is directly related to the number of qubits required. Complex variables in the unconstrained QP problem can also be handled by defining the real and the imaginary parts of each variable as two separate real variables. It effectively doubles the number of variables and, hence, the number of required qubits.

Lastly, the scope of optimization problems that quantum annealing can handle can be further extended to include *constrained* QP problems. The constraints in the problem can be accommodated by treating them as the penalty of the cost function [24]. As an instructive example, let's consider a constrained optimization problem of

Maximize
$$x^2 + 4xy + y^2$$
 subject to $x + y \le 1$
for $x, y \in \{0, 1, 2\}$. (24)

Once the range of the variable is specified, so is the variable space that satisfies the inequality. Consequently, inequality can be expressed with a set of equality values at the expense of defining additional variables. Namely, the constraint $x + y \le 1$ can be reformulated into the following equality:

$$x + y \le 1 \Leftrightarrow x + y = c \text{ for } c \in \{0, 1\}.$$
 (25)

TABLE 1. COMPARISON OF ENCODING METHODS FOR A DISCRETEVALUED VARIABLE BETWEEN 0 AND 4.

Value	One-Hot Encoding	Domain-Wall Encoding
0	N/A	0000
1	1000	1000
2	0100	1100
3	0010	1110
4	0001	1111
N/A: Not ap	plicable	

Applying the penalty method, the constrained optimization problem (24) is transformed into an unconstrained problem as

Maximize
$$x^2 + 4xy + y^2 - w(x + y - c)^2$$

for $x, y \in \{0, 1, 2\}, c \in \{0, 1\}, w \in \mathbb{R}$. (26)

The penalty weight w is often decided in a heuristic manner [24]. By applying these tricks, quantum annealing can solve not only the QUBO but also the unconstrained and constrained QP problems. Since those tricks are prepared in classical computers, this can also be regarded as a hybrid quantum-classical algorithm.

CONCLUSIONS

This work introduces quantum annealing as a computational method to solve various types of optimization problems. In Part I of this work, the key concepts for quantum annealing are introduced. While the nature of quantum annealing imposes a limitation on its applicability to binary and unconstrained problems, recent advances in conjunction with classical computers are expanding the area of applications to include discrete and constrained problems. Once discrete variables can be accommodated, continuous variables can also be treated within the precision level that is affordable with a given resource of qubit. Such an expansion of applications enables quantum annealing to address numerous electromagnetic problems. Accordingly, Part II presents the

applications of quantum annealing in various electromagnetic problems as well as the performance study of quantum annealing compared to its classical counterpart.

ACKNOWLEDGMENT

This work was supported in part by an Institute of Information and Communications Technology Planning and Evaluation (IITP) grant funded by the Korea government (MSIT) (Grant RS-2024-00393808, Efficient design of RF components and systems based on artificial intelligence, 16%), in part by the Ministry of Science, ICT and Future Planning, Korea, under the Information Technology Research Center support program (Grant IITP-2021-0-02046, 16%) supervised by the IITP, in part by the NAVER Digital Bio Innovation Research fund, funded by the NAVER Corporation (Grant 3720230040, 16%), in part by the National Research Foundation of Korea (Grants 2018R1A6A1A03025708, 16%, 2023R1A2C2004236, 16%, and RS-2023-00255442, 10%), and in part by Alchemist Project grant funded by Korea Evaluation Institute of Industrial Technology (KEIT) and the Korea Government (MOTIE) (Project Numbers 1415179744 and 20019169, 10%). The funders had no role in the design, data collection and analysis, and reporting of the study.

AUTHOR INFORMATION

Sangbin Lee (lolants55@khu.ac.kr) is a master's degree student at the Electronics and Information Convergence Engineering

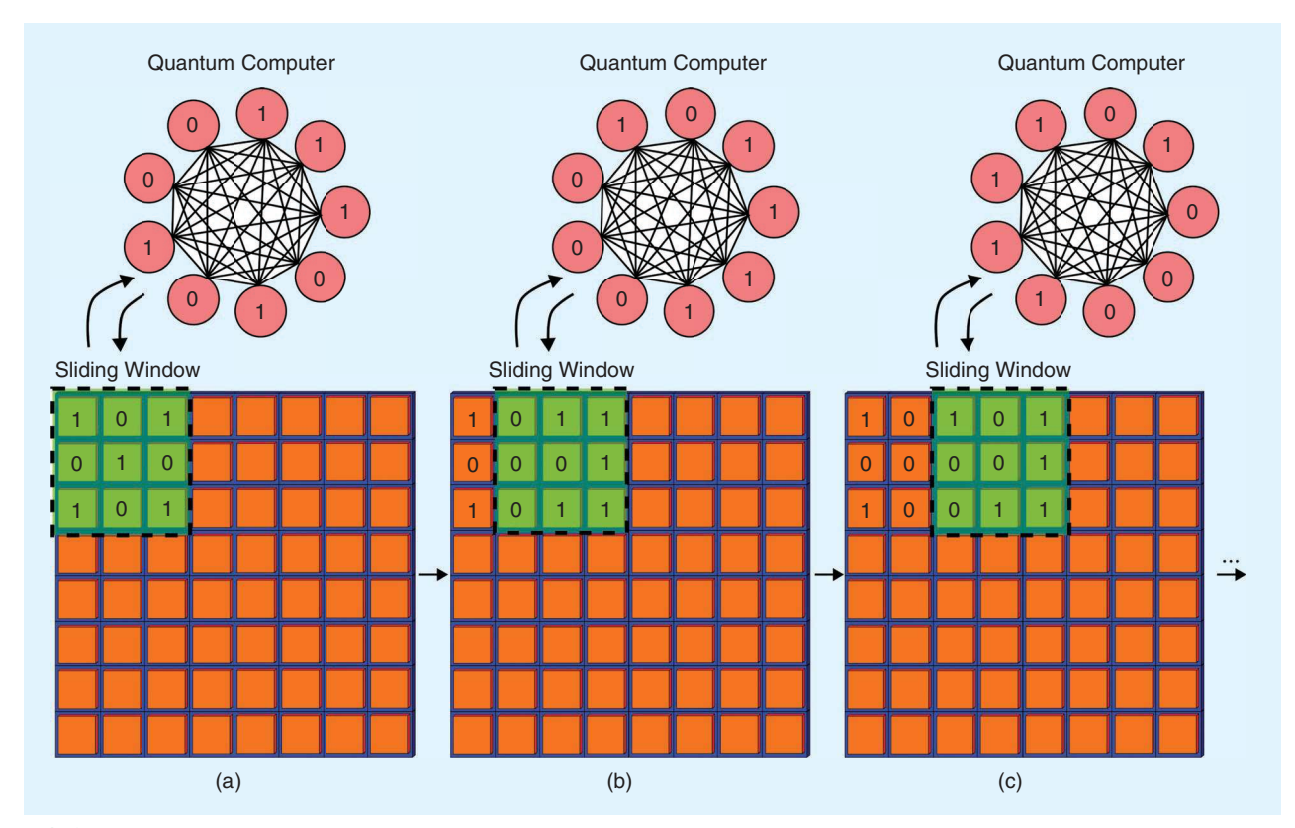


FIGURE 2. (a)-(c) An illustration of a hybrid quantum-classical algorithm for RIS beamforming applications. The orange patches represent a 1-bit reconfigurable RIS cell. A sliding window is slid across the RIS panel to solve subsections of the overall RIS panel via quantum annealing. (a) Iteration 1. (b) Iteration 2. (c) Iteration 3.

Department, Kyung Hee University, Yoingin 17104, South Korea. His current research interests include the quantum optimization for microwave and electromagnetism applications.

Qi Jian Lim (qilim2@illinois.edu) is a Ph.D. graduate student at the Department of Electrical and Computer Engineering, University of Illinois at Urbana-Champaign, Urbana, IL 61801 USA.

Charles Ross (cr26@illinois.edu) is a Ph.D. graduate student at the Department of Electrical and Computer Engineering, University of Illinois at Urbana-Champaign, Urbana, IL 61801 USA.

Eungkyu Lee (eleest@khu.ac.kr) is an assistant professor at the Electronics and Information Convergence Engineering Department, Kyung Hee University, Yoingin 17104, South Korea.

Soyul Han (asas12312195@gmail.com) is a master's degree student at the Electronics and Information Convergence Engineering Department, Kyung Hee University, Yoingin, 17104, South Korea. His current research interests include antenna and RF systems with applications in synthetic aperture radar and metasurfaces utilizing optimization techniques.

Youngmin Kim (rainmaker@keti.re.kr) is an engineer at the Hologram Research Center, Korea Electronic Technology Institute, Seoul 03924, South Korea. His current research interests include optics, including holography, visual fatigue of human vision, multimodal AI technology, and copyright protection.

Zhen Peng (zvpeng@illinois.edu) is an associate professor with the Department of Electrical and Computer Engineering, University of Illinois at Urbana-Champaign, Urbana, IL 61801 USA. His current research interests include applied and computational electromagnetics with applications in wireless communication, electronic systems, and electromagnetic scattering.

Sanghoek Kim (sanghoek@khu.ac.kr) is an associate professor at the Electronics and Information Convergence Engineering Department, Kyung Hee University, Yoingin 17104, South Korea. His current research interests include RF technology applications in wireless interfaces with bioelectronics, radar technologies, and quantum computing.

REFERENCES

- $\left[1\right]$ P. W. Shor, "Algorithms for quantum computation: Discrete logarithms and factoring," in Proc. 35th Annu. Symp. Found. Comput. Sci., Piscataway, NJ USA: IEEE, 1994, pp. 124–134, doi: 10.1109/SFCS.1994.365700.
- [2] L. K. Grover, "A fast quantum mechanical algorithm for database search," in Proc. 28th Annu. ACM Symp. Theory Comput., 1996, pp. 212-219, doi: 10.1145/237814.237866
- [3] R. P. Feynman et al., "Simulating physics with computers," Int. J. Theor. Phys, vol. 21, no. 6-7, pp. 467-488, 1982, doi: 10.1007/BF02650179.
- [4] J. Chow, O. Dial, and J. Gambetta, "IBM quantum breaks the 100-qubit processor barrier," IBM Res. Blog, 2021. [Online]. Available: https://www.ibm.com/ quantum/blog/127-qubit-quantum-processor-eagle
- [5] A. M. Childs, E. Farhi, and J. Preskill, "Robustness of adiabatic quantum computation," Phys. Rev. A, vol. 65, no. 1, 2001, Art. no. 012322, doi: 10.1103/ PhysRevA.65.012322.
- [6] C. McGeoch and P. Farré, "The advantage system: Performance update," D-Wave: The Quantum Computing Company, Tech. Rep., 2021.
- [7] N. Elsokkary, F. S. Khan, D. La Torre, T. S. Humble, and J. Gottlieb, "Financial portfolio management using D-wave quantum optimizer: The case of Abu Dhabi securities exchange," Oak Ridge National Lab.(ORNL), Oak Ridge, TN, USA, Tech. Rep., 2017.

- [8] D. Herman et al., "A survey of quantum computing for finance," 2022, arXiv:2201.02773
- [9] F. Hu et al., "Quantum computing cryptography: Finding cryptographic Boolean functions with quantum annealing by a 2000 qubit D-wave quantum computer," Phys. Lett. A, vol. 384, no. 10, 2020, Art. no. 126214, doi: 10.1016/j. physleta.2019.126214.
- [10] S. Kim, W. Shang, S. Moon, T. Pastega, E. Lee, and T. Luo, "Highperformance transparent radiative cooler designed by quantum computing," ACS Energy Lett., vol. 7, no. 12, pp. 4134-4141, 2022, doi: 10.1021/ acsenergylett.2c01969.
- [11] C. Ross, G. Gradoni, Q. J. Lim, and Z. Peng, "Engineering reflective metasurfaces with Ising Hamiltonian and quantum annealing," IEEE Trans. Antennas Propag., vol. 70, no. 4, pp. 2841-2854, Apr. 2022, doi: 10.1109/ TAP.2021.3137424.
- [12] S. Lee, S. Han, W. Song, K.-J. Lee, and S. Kim, "Discrete source optimization for microwave hyperthermia using quantum annealing," IEEE Antennas Wireless Propag. Lett., vol. 23, no. 3, pp. 1095–1099, Mar. 2024, doi: 10.1109/ LAWP.2023.3344792.
- [13] R. P. Feynman, R. B. Leighton, and M. Sands, The Feynman Lectures on Physics, Vol. III: The New Millennium Edition: Mainly Mechanics, Radiation, and Heat. New York, NY, USA: Basic Books, 2015.
- [14] R. Harris et al., "Compound Josephson-junction coupler for flux qubits with minimal crosstalk," Phys. Rev. B, vol. 80, no. 5, 2009, Art. no. 052506, doi: 10.1103/PhysRevB.80.052506.
- [15] M. W. Johnson et al., "Quantum annealing with manufactured spins," Nature, vol. 473, no. 7346, pp. 194-198, 2011, doi: 10.1038/nature10012.
- [16] S. Morita and H. Nishimori, "Mathematical foundation of quantum annealing," J. Math. Phys., vol. 49, no. 12, 2008, Art. no. 125210, doi: 10.1063/1.2995837.
- [17] R. Shankar, Principles of Quantum Mechanics. Berlin, Heidelberg, Dordrecht: Springer Science & Business Media, 2012.
- [18] S. Suzuki, J-i Inoue, and B. K. Chakrabarti, Quantum Ising Phases and Transitions in Transverse Ising Models. Berlin, Germany: Springer-Verlag, 2012. [19] A. Verma and M. Lewis, "Goal seeking quadratic unconstrained binary optimization," Results Control Optim., vol. 7, Jun. 2022, Art. no. 100125, doi: 10.1016/j.rico.2022.100125.
- [20] P. Hauke, H. G. Katzgraber, W. Lechner, H. Nishimori, and W. D. Oliver, "Perspectives of quantum annealing: Methods and implementations," Rep. Prog. Phys., vol. 83, no. 5, 2020, Art. no. 054401, doi: 10.1088/1361-6633/ab85b8.
- [21] E. Farhi, J. Goldstone, S. Gutmann, J. Lapan, A. Lundgren, and D. Preda, "A quantum adiabatic evolution algorithm applied to random instances of an np-complete problem," Science, vol. 292, no. 5516, pp. 472-475, 2001, doi: 10.1126/science.1057726.
- [22] D. Pisinger and S. Ropke, "Large neighborhood search," Eur. J. Oper. Res., vol. 206, no. 3, pp. 399-419, Sep. 2010.
- [23] J. Raymond et al., "Hybrid quantum annealing for larger-than-QPU latticestructured problems," ACM Trans. Quant. Comput., vol. 4, no. 3, pp. 1-30, 2023, doi: 10.1145/3579368.
- [24] R. M. Freund, Penalty and Barrier Methods for Constrained Optimization. Cambridge, MA, USA: Massachusetts Institute of Technology, 2004.
- [25] J. Chen, T. Stollenwerk, and N. Chancellor, "Performance of domain-wall encoding for quantum annealing," IEEE Trans. Quantum Eng., vol. 2, pp. 1-14, Jul. 2021, doi: 10.1109/TQE.2021.3094280.
- [26] K. Bharti et al., "Noisy intermediate-scale quantum algorithms," Rev. Mod. Phys., vol. 94, no. 1, Feb. 2022, Art. no. 015004, doi: 10.1103/Rev-ModPhys.94.015004.
- [27] K. Boothby, P. Bunyk, J. Raymond, and A. Roy, "Next-generation topology of D-wave quantum processors." 2020, arXiv:2003.00133.
- [28] A. W. Harrow and A. Montanaro, "Quantum computational supremacy," Nature, vol. 549, no. 7671, pp. 203-209, 2017, doi: 10.1038/nature23458.
- [29] A. Callison and N. Chancellor, "Hybrid quantum-classical algorithms in the noisy intermediate-scale quantum era and beyond," Phys. Rev. A, vol. 106, no. 1, $\label{eq:Jul.2022} \mbox{Jul. 2022, Art. no. 010101, doi: } 10.1103/\mbox{PhysRevA.} 106.010101.$
- [30] Z. Li, T. Seidel, M. Bortz, and R. Heese, "A decomposition method for the hybrid quantum-classical solution of the number partitioning problem," 2023,
- [31] F. Gao, D. Huang, Z. Zhao, W. Dai, M. Yang, and F. Shuang, "Hybrid quantum-classical general benders decomposition algorithm for unit commitment with multiple networked microgrids," 2022, arXiv:2210.06678.
- [32] T. Tran et al., "A hybrid quantum-classical approach to solving scheduling problems," in Proc. Int. Symp. Comb. Search, vol. 9, no. 1, 2016, Art. no. 18390.
- [33] Q. J. Lim, C. Ross, A. Ghosh, F. Vook, G. Gradoni, and Z. Peng, "Quantumassisted combinatorial optimization for reconfigurable intelligent surfaces in smart electromagnetic environments," IEEE Trans. Antennas Propag., vol. 72, no. 1, pp. 147-159, Jan. 2024, doi: 10.1109/TAP.2023.3298134.